Late Ediacaran Redox Stability and Metazoan Evolution

Late Ediacaran redox stability and metazoan evolution

D.T. Johnston[1], S.W. Poulton[2], T. Goldberg[3], V.N. Sergeev[4], V. Podkovyrov[5], N.G. Vorob'eva[4], A. Bekker[6], A.H. Knoll[1]

[1] Department of Earth and Planetary Sciences, Harvard University, 20 Oxford St., Cambridge MA 02138

[2] School of Civil Engineering and Geosciences, Newcastle University, Drummond Building, Newcastle upon Tyne, NE1 7RU, UK

Department of Earth Science and Engineering, Imperial College London, London, SW7 2AZ, UK

[4] Geological Institute, Russian Academy of Sciences, Moscow 109017, Russia

[5] Institute of Precambrian Geology and Geochronology, Russian Academy of Sciences, St. Petersburg 199034, Russia

[6] Department of Geological Sciences, University of Manitoba, 125 Dysart Rd., Winnipeg, MB R3T 2N2, Canada

corresponding author: (DTJ) johnston@eps.harvard.edu

Abstract: 316, Words: 6278, Figures: 7

Abstract: The Neoproterozoic arrival of animals fundamentally changed Earth's biological and geochemical trajectory. Since the early description of Ediacaran and Cambrian animal fossils, a vigorous debate has emerged about the drivers underpinning their seemingly rapid radiation. Some argue for predation and ecology as central to diversification, whereas others point to a changing chemical environment as the trigger. In both cases, questions of timing and feedbacks remain unresolved. Through these debates, the last fifty years of work has largely converged on the concept that a change in atmospheric oxygen levels, perhaps manifested indirectly as an oxygenation of the deep ocean, was causally linked to the initial diversification of large animals. What has largely been absent, but is provided in this study, is a multi-proxy stratigraphic test of this hypothesis. Here, we describe a coupled geochemical and paleontological investigation of Neoproterozoic sedimentary rocks from northern Russia. In detail, we provide iron speciation data, carbon and sulfur isotope compositions, and major element abundances from a predominantly siliciclastic succession (spanning > 1,000 meters) sampled by the Kel'tminskaya-1 drillcore. Our interpretation of these data is consistent with the hypothesis that the pO_2 threshold required for diversification of animals with high metabolic oxygen demands was crossed prior to or during the Ediacaran Period. Redox *stabilization* of shallow marine environments was, however, also critical and only occurred about 560 million years ago (Ma), when large motile bilaterians first enter the regional stratigraphic record. In contrast, neither fossils nor geochemistry lend support to the hypothesis that ecological interactions altered the course of evolution in the absence of environmental change. Together, the geochemical and paleontological records suggest a coordinated transition from low oxygen oceans sometime before the Marinoan (~635 Ma) ice age, through better oxygenated but still redox-unstable shelves of the early Ediacaran Period, to the fully and persistently oxygenated marine

environments characteristic of later Ediacaran successions that preserve the first bilaterian macrofossils and trace fossils.

1.0 INTRODUCTION

The hypothesis that increased oxygen availability facilitated Ediacaran (635-542 Ma) metazoan evolution dates back more than half a century (Cloud and Drake, 1968; Nursall, 1959). This hypothesis posits that an increase in the oxygen content of shallow-marine environments was physiologically necessary for the emergence of large, highly energetic animals (Raff and Raff, 1970; Rhoads and Morse, 1971). Ecological and physiological observations place lower dissolved oxygen (DO) limits for ocean waters in which different types of animals can live (e.g., (Diaz and Rosenberg, 1995; Levin, 2003)). They further make predictions about body shape in early animals, based on diffusion length-scales for organisms that lack a circulatory system for bulk oxygen transport (Knoll, 2011; Payne et al., 2011; Raff and Raff, 1970; Runnegar, 1991). Together, then, these physiological requirements for oxygen predict that geochemical evidence for well-oxygenated marine waters should coincide with or slightly antedate fossil records of animals with high oxygen demand.

A growing suite of redox-related geochemical tools is now available to test the oxygen-facilitation hypothesis. For instance, reconstructions of the iron and sulfur cycles in Ediacaran strata of Newfoundland suggest a broad consistency between oxygenation and animal diversification (Canfield et al., 2007). There, deep-water axial turbidites with low overall organic carbon contents preserve a shift in the distribution of iron minerals that bespeaks increased DO. This inferred change in redox structure is placed atop the ~580 Ma glacial deposit

of the Gaskiers Formation and is followed by the appearance of Ediacaran macrofossils through the overlying Drook, Briscal and Mistaken Point formations. A similar geochemical formula was applied to fossil-bearing sections from South China and the Yukon (McFadden et al., 2008; Narbonne and Aitken, 1990), however the relationship between the fossil record and redox transitions in these basins, especially as they relate to Newfoundland (Canfield et al., 2007), is less clear cut. Correlations among these basins and their stratigraphic successions are challenging, and the postulated role of sulfide as a key toxin in basins developed along the continental margin of the South China craton further complicates physiological interpretations (Li et al., 2010).

Thus, the lack of first-order geochemical coherence among these localities, perhaps due in part to locally variable biogeochemical fluxes (Johnston et al., 2010; Kah and Bartley, 2011), means that the direct role that oxygen played in the timing of both local and global animal diversification remains to be fully elucidated. Given this, it is important to acknowledge models of eumetazoan innovation that bypass oxygen entirely and call upon ecology as the primary driver (Butterfield, 2009; Peterson and Butterfield, 2005; Stanley, 1973). In addressing the role of oxygen through the application of robust geochemical techniques, both hypotheses can ultimately be tested.

Environmental and ecological hypotheses make distinct predictions about the sequence of biological and geochemical changes, which can be tested through detailed geochemical analyses of fossil-bearing Ediacaran strata. This forms the premise for our current study of Ediacaran marine sediments from the Eastern European Platform (EEP). This succession hosts some of the most exquisite examples of early animal life (Fedonkin et al., 2007; Fedonkin and Waggoner, 1997; Martin et al., 2000) and offers a prime opportunity to reconstruct oceanic redox conditions

through the application of a range of geochemical methods. Here, we thus revisit both the oxygen facilitation and ecology hypotheses through the application of iron, sulfur, and carbon geochemistry, bulk elemental data, and rigorous statistical analysis.

2.0 GEOLOGICAL SETTING

The Kel'tminskaya-1 drillhole, located near the Dzhezhim–Parma uplift in northern Russia records ~5,000 meters of upper Neoproterozoic and Paleozoic strata that accumulated along the northeast margin of the East European Platform (Fig. 1). The lowermost 2000 m of the core contains a mixed carbonate and siliciclastic succession deposited in a shallow-marine setting, correlated bio- and chemo-stratigraphically to the Cryogenian (850-635 Ma) Karatau Group in the Ural Mountains (Raaben and Oparenkova, 1997; Sergeev, 2006; Sergeev and Seong-Joo, 2006). Age constraints for this part of the succession are limited, but stromatolites, vase-shaped microfossils (Maslov et al., 1994; Porter et al., 2003) and correlation to Pb-Pb dated carbonate rocks of the Min'yar Formation in the Ural Mountains suggest an age of 780 ± 85 Ma (Ovchinnikova et al., 2000).

Unconformably overlying Cryogenian strata, and thus separated by > 100 million years, are siliciclastics of the Vychegda, Redkino and Kotlin formations. The Vychegda Formation, a 600 m thick succession, is dominated by interbedded sandstone, siltstone and shale suggestive of mid-shelf deposition. Diverse large ornamented microfossils first appear low in this unit (at 2779 m) and indicate an Ediacaran age (Vorob'eva et al., 2009b) (Fig. 1). No Sturtian or Marinoan-aged diamictites are present in the drillcore, complicating placement of the Cryogenian-Ediacaran boundary. However, typically pre-Ediacaran microfossils occur in mixed

coastal siliciclastic rocks in the lowermost six meters of the Vychegda Formation, suggesting that the period boundary is marked by a cryptic unconformity just above these beds (Vorob'eva et al., 2009a, b).

The exact duration of the proposed hiatus is unclear, however overlying Vychegda shales, interpreted as mid-shelf deposits (Vorob'eva et al., 2009a, b), contain a diverse assemblage of large, highly ornamented organic-walled microfossils akin to the Ediacaran Complex Acanthomorph-dominated Palynoflora (ECAP (Grey, 2005)). In central and southern Australia (Grey and Calver, 2007; Grey et al., 2003), the ECAP assemblage populates a restricted temporal interval, occupying beds that overlie the ca. 580 Ma Acraman impact layer, but underlie the strongly negative C-isotopic excursion of the Wonoka Formation (correlated with the Shuram anomaly in Oman). Well above this interval, diverse Ediacaran macrofossils appear. The same is true in China (Jiang et al., 2007; McFadden et al., 2008), Subhimalayan India (Kaufman et al., 2006), and the Patom region of Siberia (Pokrovskii, 2006; Sergeev et al., 2011). Detrital zircons also constrain ECAP acritarchs in the Hedmark Group, Norway to be younger than 620+/-14 Ma (Bingen et al., 2005), consistent with other results. Taken together, these observations most conservatively suggest that the Vychegda Formation was deposited during the Ediacaran Period, before 558 Ma, a U-Pb constraint provided from the Redkino Formation and discussed below. Given the distribution of ECAP microfossils elsewhere, we suggest that the majority of Vychegda Formation deposition took place between 580 and 558 Ma.

Siliciclastic rocks in the upper 1000 m of the Kel’tminskaya-1 drillhole correlate with the Redkino and Kotlin successions preserved across the EEP (Sokolov and Fedonkin, 1990). Redkino rocks lack highly ornamented microfossils but preserve an exceptional record of Ediacaran macrofossils, including *Kimberella*, widely considered to be the earliest known

bilaterian animal (Fedonkin et al., 2007; Fedonkin and Waggoner, 1997) (Fig. 1). Additional information about the paleobiology of Kel'tminskaya-1 core material can be found in (Vorob'eva et al., 2009a, b). U-Pb dates on zircons in Redkino ash beds indicate ages of 555.3 ± 0.3 Ma near the top of the succession (Martin et al., 2000) and 558 ± 1 Ma toward its base (Grazhdankin, 2003). Biostratigraphy places the Proterozoic-Cambrian boundary at or near the top of the Kotlin succession.

3.0 METHODS

Iron speciation was performed following a calibrated extraction technique (Poulton and Canfield, 2005). This method targets operationally defined iron pools, such as iron carbonate (Fe_{carb}: ankerite and siderite), Fe^{3+} oxides (Fe_{ox}: goethite and hematite) and mixed valence iron minerals (Fe_{mag}: magnetite). Pyrite iron (Fe_{py}) and sulfur, as well as acid volatile sulfur (AVS; below detection in these samples) were extracted via traditional distillation techniques (Canfield et al., 1986). Together, these pools define a suite of minerals that can be considered biogeochemically available, or highly reactive (FeHr) towards reductive dissolution in surface and near-surface environments ($FeHr = Fe_{carb} + Fe_{ox} + Fe_{mag} + Fe_{py}$) (Poulton et al., 2004a). Total Fe (FeT) additionally comprises a largely unreactive silicate iron pool (FeU), delivered to the marine environment via weathered detrital fluxes (i.e., FeHr + FeU = FeT). Both pools are classically defined in relation to their reactivity toward dissolved sulfide (Canfield et al., 1992; Poulton et al., 2004b). Total Fe contents were derived from both HF-$HClO_4$-HNO_3 extractions and standard XRF analyses. X-ray fluorescence also provided major element chemistry, most

149 notably Al, Ti, K, Na, Si, Mg, Mn, and P (performed at UMass Amherst). All aqueous Fe
150 analyses were performed by AAS, with a RSD of <5% for all stages.

151 Sulfur isotope analyses were performed by combusting sulfide precipitates (see Fe_{py}
152 above) to SO_2 and then run via continuous-flow on a Thermofinnigan Delta V with an analytical
153 reproducibility of 0.2‰, normalized to VCDT. Carbon isotopes were performed on splits of the
154 same bulk sample. Prior to carbon isotope analyses, samples were decalcified with a 10% HCl
155 pre-treatment. Decalcified samples were analyzed for organic carbon isotopes ($\delta^{13}C_{org}$) and total
156 organic carbon contents (TOC) via combustion to CO_2 with a Carlo Erba EA interfaced with a
157 Thermofinnigan Delta V configured in continuous flow mode. Samples were run in duplicate
158 with reproducibility of 0.2‰ and <0.05 wt%. Carbonate carbon isotope values ($\delta^{13}C_{carb}$) were
159 measured on a Dual Inlet VG Optima gas source mass spectrometer interfaced with an Isocarb
160 prep device. Reproducibility is roughly 0.1‰ and all carbon isotope data are normalized to a
161 VPDB scale.

162

163 ## 4.0 RESULTS AND DISCUSSION

164 We used iron speciation chemistry, major element abundances, and stable carbon and
165 sulfur isotopic ratios to characterize oceanic redox conditions and biogeochemical cycling during
166 deposition of the Kel'tminskaya-1 succession (Fig. 2). The distribution of reactive iron minerals
167 in marine sediment has been calibrated in order to differentiate between oxic and anoxic water
168 column conditions (Canfield et al., 1996; Lyons et al., 2003; Poulton and Canfield, 2011;
169 Raiswell et al., 1988; Raiswell and Canfield, 1996; Raiswell et al., 1994; Raiswell et al., 2001).
170 In keeping with these calibrations, we interpret highly reactive iron (FeHr)/total iron (FeT) >

0.38 as diagnostic of anoxia, with Phanerozoic and modern marine FeHr/FeT values of 0.14±0.08 and 0.26±0.08 falling within a range characteristic of an oxic depositional environment (Anderson and Raiswell, 2004; Poulton and Raiswell, 2002; Raiswell and Canfield, 1998). Fe/Al provides additional paleoredox information, with the added value of circumventing dilution effects related to carbonate contents (Lyons et al., 2003). In the case of Fe/Al (here Fe refers to FeT), crustal values of ~0.5-0.6 commonly characterize oxic conditions, with anoxia generally giving rise to Fe/Al enrichments above this threshold (Lyons and Severmann, 2006).

We also report the chemical index of alteration (CIA) for siliciclastic samples in order to monitor the nature and maturity of terrigenous fluxes into the basin (Nesbitt et al., 1997; Nesbitt and Young, 1984; Nesbitt et al., 1996; Tosca et al., 2010). CIA, a measure of the degree of weathering, is expressed as $Al_2O_3/[Al_2O_3 + CaO + Na_2O + K_2O]$. Given the importance of clay minerals in organic matter burial and early diagenetic biogeochemistry (Hedges and Keil, 1995; Keil et al., 1994; Rothman and Forney, 2007), we provide these data to assay potential changes in source terrain for detrital siliciclastics that would in turn effect marine geochemical cycling, all presented against the backdrop of previous work on the Neoproterozoic (Kennedy et al., 2006; Tosca et al., 2010). Finally, reporting on the isotopic composition and abundances of carbon and sulfur allows the geochemical measures described above to be linked more directly to biogeochemical cycling. That is, the stoichiometry of heterotrophic remineralization reactions provides a means of relating organic carbon (and factors associated with production, export and burial) to electron accepting species within the Fe and S cycles (Fe-oxides and sulfate, in particular). Below we discuss the distribution of these data in the context of their specific geological setting, beginning with the oldest, Cryogenian-age samples. The full data are presented in the supplemental materials.

194

195 **4.1 Cryogenian records from the EEP**

196 Geochemical data for the carbonate-rich Cryogenian portion of the Kel'tminskya-1
197 drillhole mirror those of pre-Sturtian successions elsewhere (Canfield et al., 2008; Johnston et
198 al., 2010). Within the lower reach of the drillhole, $\delta^{13}C_{carb}$ varies stratigraphically from -4‰ to
199 4‰, consistent with earlier Neoproterozoic values from the Uralian Karatau Group (Podkovyrov
200 et al., 1998) and correlative carbonates on the Siberian Platform (Bartley et al., 2001). Organic
201 carbon content is generally low (< 0.4 wt%), and on average is higher in Cryogenian than in
202 younger intervals of the succession; $\delta^{13}C_{org}$ values for carbonate-rich Cryogenian samples vary
203 moderately around a mean of about -29‰. A monotonic ~ 8‰ rise in $\delta^{13}C_{carb}$ through the
204 Vapol' Formation may suggest an increase in organic carbon burial (Hayes et al., 1999), but a
205 tight, parallel change in $\delta^{13}C_{org}$ is lacking. This lack of isotopic covariance is not uncommon in
206 Neoproterozoic carbonates (Fike et al., 2006; Swanson-Hysell et al., 2010), with recent work
207 pointing to complexities associated with $\delta^{13}C_{org}$ as masking classic carbon isotope behavior
208 (Johnston et al., 2012; Knoll et al., 1986). In the case of the Cryogenian from Russia, the data
209 reported here support a stratigraphic link to the Ural Mountains and provide yet another example
210 of a pre-Sturtian carbon cycle with a large degree of variability. That is, the biogeochemical
211 picture provided by the Vapol' and Yskemess formations is consistent with those preserved
212 globally.

213 The Vapol' and Yskemess formations are carbonate dominated, with, on average, a
214 weight percent total iron (Fig. 2), much of which occurs as Fe-carbonate. The iron carbonate
215 fraction was determined via the first step of the normal Fe-speciation method, which is a weak

acid extract defined to access carbonate phases (ankerite and siderite). The further application of Fe-speciation data requires added discussion. It is important to appreciate that Fe-speciation methods are calibrated on fine-grained siliciclastic sediments and the threshold values that guide the reading of these metrics are similarly rooted. This, of course, complicates the direct and literal interpretation of Fe-speciation data on carbonates. However, a number of points require consideration. Foremost, the determination of iron carbonate, simply as a mass fraction and as presented above, is robust. Next, the logic of Fe speciation methods is based on the precipitation of Fe minerals under anoxic water column conditions and the subsequent settling of these minerals, enriching local sediments. This iron enrichment is only possible when bottom water conditions are anoxic. Thus, iron enrichment should occur in anoxic carbonate-rich environments in the same fashion as it does in siliciclastic sediments, provided that there is a reasonable amount of total Fe to source. Fe enrichment in carbonates can occur because of water column Fe precipitation or suspended load siliciclastic admixture. (Fe/Al ratios for carbonates were not measured due to interferences associated with high [Ca^{2+}], a function of carbonate content.) Nonetheless, where FeT is high, as is the case with the EEP carbonates (FeT averages ~1.3 wt%), the potential for minor Fe mobilization and redistribution following deposition should not result in a spurious redox signal, and its association with carbonates suggests that it is reactive iron as opposed to silicate iron or iron delivered with detrital fluxes. With the discussion above and in noting that Fe in ancient carbonates usually stays close to original depositional values (Tucker and Wright, 1990), Fe speciation has been successfully applied in a variety of siliciclastic-poor settings (e.g. (Goldberg et al., 2005; Kendall et al., 2010; Marz et al., 2008). However, although we argue that the Fe-speciation proxy should generally behave similarly in carbonate-rich and siliciclastic rocks (also see (Poulton and Canfield, 2005)), we do

not require the strict interpretation of carbonate iron data for the story forwarded here. We simply present iron data from a limited Cyrogenian dataset against the backdrop of contemporaneous siliciclastic units from North America, which is discussed below.

Iron speciation data for the Vapol' and Yskemess formations are variable but suggest a highly reactive iron enrichment (and inferred bottom water anoxia), even though most of these rocks were deposited in no more than a few tens of meters of water. Calculated 95% confidence intervals for FeHr/FeT in the Vapol' and Yskemess are $0.54^{0.04}_{1.21}$ and $0.48^{0.12}_{0.79}$, respectively (see also Fig. 2, 3). For the samples with elevated reactive iron contents, low sulfide contents (Fig. 2) result in low Fe_{py}/FeHr ratios (~0.1), which, coupled with an Fe speciation signal that is Fe_{carb} dominated (Figure 3), points to anoxic ferruginous water column conditions (Poulton et al., 2004; Poulton and Canfield, 2011) for nearly 80% of the Cryogenian samples. As noted above, these data simply provide a complementary picture. Interestingly, however, and in support of using Fe methods on carbonates, correlative successions from other continents also feature low pyrite contents and signatures of anoxia. For example, by almost every metric, the EEP results are consistent with the shale-dominated Chuar Group in the Grand Canyon, USA (Johnston et al., 2010). There, a stratigraphically resolved data-set records persistent subsurface water column anoxia, in waters of similar depth, with only modest sulfide production corresponding to intervals of increased TOC burial. Given the dominant role of the atmosphere (and the O_2 reservoir) in disseminating oxygen into the surface mixed layer of the ocean, anoxia on the shelf likely reflects lower O_2, noting that local biogeochemistry can influence the DO load (Johnston et al., 2010).

4.2 Ediacaran records from the EEP

Geochemical data from the siliciclastic Ediacaran portion of the Kel'tminskya-1 drillhole (above 2779m) suggest a more fully oxygenated water column, as well as an increasing trend toward redox stability moving upward through the section. Total iron abundances for the Vychegda, Redkino and Kotlin formations are significantly higher than for the carbonate-rich Cryogenian section, as expected for a shale-dominated succession, with Fe and P concentrations similar to average Phanerozoic shale contents (~5 wt% and 0.07 wt %, respectively; Fig. 2) (Turekian and Wedepohl, 1961). The distribution of reactive iron phases from the EEP suggests a markedly more oxygenated depositional environment for the Ediacaran shales than for the underlying Cryogenian deposits. Ediacaran FeHr/FeT values oscillate around a mean of $0.26^{0.13}_{0.36}$ (95% confidence interval), similar to that characteristic of modern oxic marine sediments (Fig. 2, 3) (Poulton and Canfield, 2011; Poulton and Raiswell, 2002).

Although suggesting more oxygenated conditions, in detail the chemical variability in the Vychegda Formation does allow (and may indicate; (Poulton and Canfield, 2011)) recurring intervals of less oxygenated bottom waters, which were replaced by more persistently oxygenated conditions by Redkino time. Along those lines, a closer look at the data reveals an important change *within* the Ediacaran portion of the succession. Notably, the Vychegda-Redkino sequence boundary separates distinct geochemical regimes (Fig. 2). Thus, we subdivide the Ediacaran stratigraphy into the earlier Ediacaran interval (~580 to 558 Ma) represented by the Vychegda Formation above 2779m and the upper Ediacaran interval (~558 to 542 Ma) recorded by the Redkino-Kotlin formations. As depicted in Figure 3, many of the reported geochemical metrics from the early and late Ediacaran successions scatter around similar average values, but early Ediacaran samples consistently show more variability. Our data, thus, present a

284 picture of a shelf environment that gradually evolved from one of significant redox heterogeneity
285 in the Cryogenian, through a more oxygenated but still unstable redox regime in the early
286 Ediacaran, to a stable, persistently oxygenated state in the late Ediacaran.

287 In the context of this interpretation, we can consider implications for local
288 biogeochemical cycling. As posited earlier, atmospheric oxygen is one of a few levers on
289 bottom water chemistry, acknowledging that heterotrophy following TOC loading and the
290 ensuing benthic fluxes represent a significant local sink for oxidants (Johnston et al., 2010). To
291 evaluate these contrasting mechanisms, we investigate the relationship between the carbon,
292 phosphorus and iron budgets inferred from Kel'tminskaya-1 samples. The EEP shale is
293 generally TOC lean (Fig. 2, 5), contains typical P contents, and low overall pyrite concentrations.
294 The low observed pyrite contents suggest that dissimilatory sulfate reduction (Canfield, 2001)
295 was not a prominent remineralization pathway in these settings. Without sulfate, this leaves
296 oxygen, nitrate and iron oxides as potentially prominent electron acceptors. The ratio of TOC to
297 reactive iron does not reveal a significant linkage (Fig. 5); however, the conversion of originally
298 mixed valence Fe inputs to predominantly ferrous iron carbonate does require a reductive
299 catalyst, which most naturally would be dissimilatory iron reduction (Fig. 5a). As an extension,
300 the efficiency of P burial relative to organic C can provide important information about
301 preferential P regeneration through remineralization reactions under different redox conditions
302 (Algeo and Ingall, 2007; Ingall and Jahnke, 1994). This often results in a strong positive
303 correlation between C and P, and high organic C:P under anoxic conditions (cf. (Jilbert et al.,
304 2011; Kraal et al., 2010). For example, organic C:P in modern anoxic settings can exceed 300,
305 but deposition under fully oxygenated modern conditions often drive organic C:P below 50
306 (Algeo and Ingall, 2007). In the case of the EEP, organic C:P ratios are consistently low,

approaching 1:1 for the Vychegda and ~2:1 for the Redkino and Kotlin formations (Fig. 5b). Low organic C:P ratios, coupled with low total organic C and the lack of an authigenic P enrichment above that of normal marine shale, is often interpreted as a result of a higher redox potential in the local environment, consistent with an oxygenated water column (Algeo and Ingall, 2007).

The distinction between early and late Ediacaran geochemistry can be investigated more quantitatively. To explore the robustness of this partitioning, we bootstrapped a Monte Carlo resampling (n = 1000) of the Vychegda – Redkino/Kotlin data sets (n = 35 and 44, respectively). This approach clearly identifies differences in Fe/Al ratios and pyrite $\delta^{34}S$ values, with CIA values holding steady near a value of 0.70 (Fig. 6). Interestingly, the average FeHr/FeT value differs little between lower Ediacaran Vychegda shales and those of the overlying Redkino-Kotlin succession (Fig. 6a); however, the upper and lower Ediacaran successions differ in the distribution of FeHr/FeT values about the mean, indicating a marked *stabilization* of the redox environment by the late Ediacaran. Whereas the earlier Ediacaran samples record highly variable bottom water conditions, younger Ediacaran shales document a stable and persistently oxic seafloor. This up-section change in FeHr/FeT distribution does not necessarily require an increase in the dissolved oxygen content of seawater, although increasing oxygen provides a ready mechanism for increased redox stability. Fe/Al values also closely track this shift (Fig. 6), and in the absence of apparent change in other possible controls on FeT, these data point toward a broadly oxygenated environment throughout the entire interval of the Ediacaran Period sampled by the drillcore (cf. (Lyons and Severmann, 2006; Lyons et al., 2003; Severmann et al., 2008)). Similarly, more variability in Fe/Al ratios in the early Ediacaran, in part perhaps related to FeT, reflects a greater degree of redox instability, which is again succeeded by stable and

oxic-like Fe/Al ratios in the younger Ediacaran part of the succession. Finally, the CIA values of these two populations are similar (Fig. 5), and thus the chemical maturity of terrigenous clay inputs can also be taken as roughly constant, ruling out major change in the terrestrial weathering regime as a driver of the observed geochemical stabilization (Kennedy et al., 2006; Tosca et al., 2010). As clay minerals provide a critical template for the proficient burial of organic matter, it is important to place constraints on this vector. This is especially true considering that the inception of pedogenic clay formation was proposed as a spur for Ediacaran changes in organic burial and associated oxygen production (Kennedy et al., 2006). The absence of a change in the chemical composition of weathered material and sedimentation rate (as reflected by a persistent and similar depositional setting) indicates that there was no major change in provenance or composition of sediments entering the EEP basin.

Our data thus indicate that by the time that the main Vychegda sequence began to deposit, marine redox conditions had changed from persistent anoxia to a broadly oxygenated water column. This conclusion, of course, reflects oceanographic conditions in a single basin and does not preclude earlier oxygenation of water masses elsewhere. That noted, data from other continents similarly record a redox transition within the lower part of the Ediacaran Period (Canfield et al., 2007; Fike et al., 2006; Scott et al., 2008; Shen et al., 2008). Where the EEP data extend our understanding is their recording of redox *stabilization*, perhaps at ca. 560 Ma. Neither redox transition nor redox stabilization require that pO_2 reached modern levels in the Ediacaran – indeed, both data and models suggest that present day pO_2 was first reached only in the later Paleozoic Era (Bergman et al., 2004; Berner and Canfield, 1989; Dahl et al., 2010). Rather they suggest that, perhaps for the first time in Earth history, oxygen levels were sufficient to limit the spread of anoxia in shallow water settings.

353

354 **4.3 Insight from the sulfur cycle**

355 The sulfur cycle is sensitive to the oxygen content of the atmosphere, and as such, may
356 provide a test of proposed mid-Ediacaran transitions (cf. (Berner and Canfield, 1989; Claypool et
357 al., 1980; Garrels and Lerman, 1981)). We first look at the limited data from the Cryogenian
358 Vapol' and Yskemess formations. Here, $\delta^{34}S$ values are highly variable and range from above
359 estimates of contemporaneous seawater sulfate (Johnston et al., 2010) to almost -30‰. Scaling
360 loosely with TOC content (Fig. 7b), the 50‰ range certainly reflects primary microbial
361 contributions from sulfate reduction and may also indicate sulfur disproportionation reactions
362 (Canfield and Teske, 1996; Johnston et al., 2005), although mass-balance effects of local sulfate
363 limitation might also have been in play (Canfield, 2001; Hayes, 2001). Although the data
364 exhibit some scatter, in particular where TOC values are higher, $\delta^{34}S$ values are generally more
365 enriched, consistent with sulfate limitation within the sediments and, consequently, near-
366 quantitative reduction of pore-water sulfate.

367 The sulfur isotopic composition of pyrite from the Ediacaran portion of the EEP is also
368 quite variable. The $\delta^{34}S$ values of pyrite within the Vychegda Formation are, on average, more
369 depleted and variable than sulfides from the overlying Redkino and Kotlin formations (a mean
370 value of 2‰ as opposed to 12‰ for the late Ediacaran; Fig. 6d). Importantly, the Vychegda
371 Formation is also more pyrite-rich than overlying strata, averaging ~0.08 and ranging up to 0.3
372 wt% pyrite (the Redkino and Kotlin formations average ~0.02 wt%). If we presume a $\delta^{34}S$ of
373 seawater sulfate between 20‰ and 30‰, similar to estimates from early Ediacaran successions
374 in Oman, Namibia, South China and Australia (Fike et al., 2006; Halverson and Hurtgen, 2007;

Hurtgen et al., 2002; Hurtgen et al., 2006; McFadden et al., 2008), then the net fractionation associated with a consortium of microbial metabolisms only requires the influence of sulfate reduction. If the Ediacaran seafloor was moving toward a more oxygenated state, as suggested by iron speciation data, then an oxidative sulfur cycle was almost certainly present in the water column. Emerging tools, specifically the minor sulfur isotopes (Johnston, 2011), may provide a test of this interpretation and allow for the isotopic contributions of reductive and oxidative processes to be more uniquely constrained.

The overlying Redkino and Kotlin formations contain much less pyrite and preserve sulfur isotope compositions that cluster toward more enriched values. Although not as enriched as the super-heavy pyrites observed elsewhere (Ries et al., 2009), values are almost always positive (> 0‰). Limited data (Fike and Grotzinger, 2008; Fike et al., 2006; Kampschulte and Strauss, 2004) and a model treatment of that data (Halverson and Hurtgen, 2007) suggest an enrichment in the $\delta^{34}S$ of seawater sulfate toward the end of the Ediacaran, although more recent datasets suggest seawater sulfate remained near 20‰ at that time (Ries et al., 2009). The lack of consistency among these data is curious, as it points to either the infidelity of certain proxies, poor absolute correlation between continents, or – perhaps most likely – a heterogeneous seawater sulfate reservoir. Regardless of the reason, this variability makes the diagnosis of the Redkino and Kotlin sulfur cycle difficult. If sulfate was becoming more ^{34}S enriched at that time, then the net fractionation between sulfate and sulfide may not have changed significantly from that observed in the underlying Vychegda Formation. However, if sulfate remained largely invariant, these data suggest that the net fractionation decreased drastically. This later scenario could reflect an extreme deficiency in seawater sulfate concentrations (Habicht et al., 2002), but is more likely associated with simple sulfate limitation within the sediments. The latter

interpretation is consistent with other geochemical proxies in suggesting that, regionally, anoxia developed only within the sediment column.

4.4 Incorporating biological considerations

Geochemistry divides the Kel'tminskaya-1 record into three parts: a pre-Ediacaran (Cryogenian) portion recording the common occurrence of ferruginous water masses in shallow-water environments; a lower Ediacaran succession documenting more oxygenated, but still fluctuating bottom-water conditions on the shelf, and an upper Ediacaran interval that records a fully and persistently oxic water column. Fossils divide regional stratigraphy in much the same fashion (Fig. 1, 2): the Cryogenian rocks are characterized by a modest diversity of protists (Vorob'eva et al., 2009a), recording microscopic eukaryotes that could thrive at low pO_2. In contrast, the upper Ediacaran (Redkino-Kotlin) succession contains macroscopic animals, as well as trace fossils (Fedonkin et al., 2007; Fedonkin and Waggoner, 1997). In between lie the diverse, large ornamented microfossil assemblage characteristic of lower Ediacaran successions worldwide (Vorob'eva et al., 2009a). Data on morphology, wall ultrastructure, size frequency distribution and preserved intracellular contents suggest that many of these distinctive microfossils represent egg and diapause cysts of early animals (Cohen et al., 2009; Sergeev et al., 2011; Yin et al., 2007). Modern animals produce resting stages when fertilized eggs have a high probability of landing where growth is difficult or impossible (Cohen et al., 2009); therefore, it makes physiological sense that the Ediacaran cysts should be abundant and diverse in basins where geochemical data indicate bottom water redox instability. Whether animal or something else, the abundance of these cysts in Vychegda Formation shale indicates that environmental

conditions were frequently inimical to growth. Few if any of these microfossils persist into beds marked by persistently oxic water column conditions. The hypothesis that the early Ediacaran seafloor was intermediate in redox character to its pre-Ediacaran and late Ediacaran counterparts is also consistent with the presence of moderately differentiated but essentially two-dimensional macrofossils in earlier Ediacaran shales from China (Yuan et al., 2011).

Diverse macroscopic animals first appear regionally in Redkino-aged deposits (Sokolov and Fedonkin, 1990; Sokolov and Iwanowski, 1990). Many of these appear to have a simple anatomy, and may largely represent bodyplans in which upper and lower epidermis enclose inert, mesoglea-like material (e.g., (Sperling and Vinther, 2010)). One body-fossil population, however, is widely regarded as the remains of a bilaterian animal. *Kimberella quadrata* was a roughly 2 cm long and at least 1 cm thick organism whose fossil impressions show a distinct anterior-posterior axis with a plane of symmetry running from front to back (Fedonkin et al., 2007). It is occasionally preserved at the end of a trace fossil that documents directional movement across the sediment surface and sometimes also occurs with anterior scratch marks similar to those made by the radulae of mollusks during feeding (Fedonkin et al., 2007). While the precise phylogenetic relationships of *Kimberella* remain open to question, it has a strong claim to status as a bilaterian animal and almost undoubtedly would have required more oxygen for physiological function than other commonly preserved Ediacaran macroorganisms. Independently of *Kimberella*, and consistent with the predictions of molecular clocks (Erwin et al., 2011), trace fossils in the Redkino succession indicate a modest diversity of bilaterian animals. Thus, in the EEP, geochemical evidence for stabilization of pervasively oxic conditions in shelf environments correlates with the appearance of animals with unprecedentedly high oxygen demand.

443 The statistical treatment presented in Figure 6 helps further explain why the Vychegda
444 and Redkino/Kotlin intervals should be characterized by life cycles with resting stages and large,
445 highly energetic animals, respectively. While neither succession displays Fe-speciation evidence
446 for strong water mass anoxia, and while the mean value of FeHr/FeT is similar for the two
447 intervals, the greater dispersal about the mean for Vychegda samples results in nearly half of all
448 values falling within the 'equivocal' redox range; Redkino/Kotlin samples do not record such a
449 FeHr enrichment. In a recent review, it has been postulated that these intermediate FeHr/FeT
450 values (from 0.26-0.38 in FeHr/FeT) point toward "possible anoxia" (Poulton and Canfield,
451 2011). The term "dysoxia" is commonly frowned upon by geochemists because conditions of
452 low (but measurable) DO are not demarcated by a reliable geochemical fence. Biologists, in
453 contrast, pay close attention to dysoxic/hypoxic waters because their low oxygen contents (less
454 than 1-2 ml/l) strictly limit animal size, locomotion and diversity (e.g., (Diaz and Rosenberg,
455 1995; Seibel and Drazen, 2007; Vaquer-Sunyer and Duarte, 2008)). Hypoxia during the
456 deposition of the Vychegda Formation may have been sufficiently frequent to favor small
457 animals able to survive episodic bottom water anoxia as well as other unfavorable conditions by
458 forming resting cysts. The removal of this limitation, then, correlates with the first appearance of
459 large, thick, highly motile animals.

460 In combination, then, geochemical and paleontological data from northwestern Russia are
461 fully consistent with the hypothesis that evolving redox conditions exerted a strong influence on
462 the timing of early animal evolution. What about contrasting ecological hypotheses? Few would
463 dispute that ecology played an important role in animal diversification (Butterfield, 2007; Knoll,
464 1994), but what geochemical and paleontological features are uniquely predicted by this
465 hypothesis? The ornamentation of large Ediacaran microfossils have been interpreted as a

466 defensive response to bilaterian predators (Peterson and Butterfield, 2005), but no bilaterian
467 macrofossils have been found in Russian or other rocks that contain these ornamented
468 microfossils, and as bilaterians begin to populate the fossil record, the microfossils largely
469 disappear. Geochemically, ecological reorganization in a physiochemically stable ocean should
470 be reflected in changes in biogeochemical cycling across the Vychegda-Redkino boundary
471 (Butterfield, 2009; Logan et al., 1995). For instance, changes in the articulation of the biological
472 pump (Butterfield, 2009) would carry direct consequences for carbon export, organic matter
473 burial and preservation, and possibly even the type of organic compounds preserved in the
474 sediments. As recorded on the EEP, however, neither TOC nor $\delta^{13}C_{org}$ values change
475 significantly across this boundary; nor do pyrite contents or S:C ratios. The sulfur isotopic
476 composition of pyrite does record mid-Ediacaran change (Fig. 2, 6, 7), and, like other proxies,
477 records much less variability in the later Ediacaran. The more positive $\delta^{34}S$ values found for
478 younger Ediacaran pyrites may simply be another consequence of redox evolution, as sulfate
479 reduction increasingly became restricted to lower and lower horizons within the sediment
480 column, which could have facilitated the net quantitative reduction of pore-water sulfate. The
481 fossil record indicates that evolving animals drove ecological change, especially in the
482 Cambrian, when diverse new bodyplans populated the oceans (Bengston and Morris, 1992);
483 however, available data provide little support for Ediacaran ecological reorganization outside of
484 the context of changing physiochemical conditions.

485

486 5.0 CONCLUSIONS

Geochemical reconstructions of Cryogenian and Ediacaran successions on the margin of the Eastern European Platform preserve a history of Earth surface evolution that can be related to similar reconstructions from other continents (Canfield et al., 2007; Johnston et al., 2010; McFadden et al., 2008; Shen et al., 2008), and, more importantly, extends our understanding of how atmospheric oxygen may have influenced the early diversification of metazoans. Previous geochemical models have qualitatively linked proposed increase in the dissolved oxygen content of the ocean with the appearance of macroscopic animals, and although tight constraints on absolute pO_2 remains elusive, data from the EEP suggests that the redox stabilization of the local marine depositional environment may be equally important. This does not preclude a role for changing pO_2 as a means of driving stabilization, although any such mid-Ediacaran change could have been quite modest. A better understanding of absolute pO_2 trajectory may be possible through high-resolution reconstructions of marine depositional environments with high TOC loading (for instance, the Ediacaran successions of the Wernecke and Mackenzie Mountains in the Yukon, Canada), which in contrast to the EEP, would provide a more prominent oxidant sink in the bottom waters and further insight into biogeochemical cycling.

In the Kel'tminskaya-1 drillhole, unconformities separate three paleontologically and geochemically defined packages, limiting inferences about the timing, rate, and mechanisms underlying these redox state transitions. That noted, the paleontological progression recorded in northern Russia characterizes Neoproterozoic successions observed globally. The oldest macroscopic animals occur in 565-579 Ma strata from Newfoundland (Narbonne, 2005), a deep-water succession that records a stably oxic seafloor (Canfield et al., 2007) predating Redkino deposition by up to 20 million years. Quite possibly, the fossiliferous Newfoundland rocks record a time interval missing on the EEP along the Vychegda-Redkino sequence boundary. It is

510 also possible, however, that redox stability was not imposed synchronously across the globe
511 (Kah and Bartley, 2011). Indeed, protracted Ediacaran increases in pO_2 might have oxygenated
512 basins regionally, one after another, with biological changes following suit as environmental
513 conditions allowed. This hypothesis can be tested by integrated sequence stratigraphic,
514 paleontological, geochemical, and geochronological analyses of Ediacaran successions.

515 By themselves, however, paleontological and geochemical data from the northeastern
516 EEP support two first-order conclusions. First, as evidenced by a growing body of FeHr/FeT
517 data, the oft-cited Neoproterozoic 'oxygenation' does not appear to be associated with the
518 Shuram anomaly, as iron speciation data suggests an earlier arrival of this oxidizing capacity and
519 cannot speak to the rate of change (gradual versus abrupt). Continued study of Cryogenian
520 records will help to identify and describe the anatomy of this oxygenation, were a profound
521 change in atmospheric chemistry to exist. Whatever the answer, the participation of oxygen in
522 the atmospheric carbon cycle (as it interacts with critical greenhouse gasses, namely CO_2 and
523 CH_4) suggests a relationship between Neoproterozoic pO_2 and low-latitude Cryogenian
524 glaciations (Hoffman et al., 1998). Second, and most important for biological records, by about
525 580-560 Ma, redox stability came to define shallow marine seafloor environments, possibly (but
526 not necessarily) reflecting a further increase in pO_2. Our data thus most closely support the
527 classic hypothesis that increasing atmospheric oxygen paved the way for the global expansion of
528 bilaterian macrofossils, but underscores the role of redox *stability* in potentiating end-Proterozoic
529 evolutionary events.

530

Acknowledgements: We appreciate early and ongoing discussions with P. Cohen, N. Tosca, B. Gill and E. Sperling. D. Schrag and G. Eischeid are thanked for laboratory assistance. This work was funded by the Harvard Microbial Sciences Initiative (DTJ), NASA Exobiology (DTJ, AHK) and the Astrobiology Institute, MIT node (DJ and AHK), NERC (SWP), RBBR grant 10-05-00294 (VNS and NGV), and NSERC Discovery (AB).

Figure 1: A map of the Timan Ridge area showing the location of the Kel'tminskaya-1 drillhole on the northeastern margin of the Eastern European Platform (see arrow on the inset for the location on the Eastern European Platform). At right, a cartoon timeline of the characteristic fossils found in Cryogenian and Ediacaran rocks; protistan assemblages (Porter et al., 2003) are replaced by large ornamented microfossils, which gave way to complex animals (e.g. *Kimberella*).

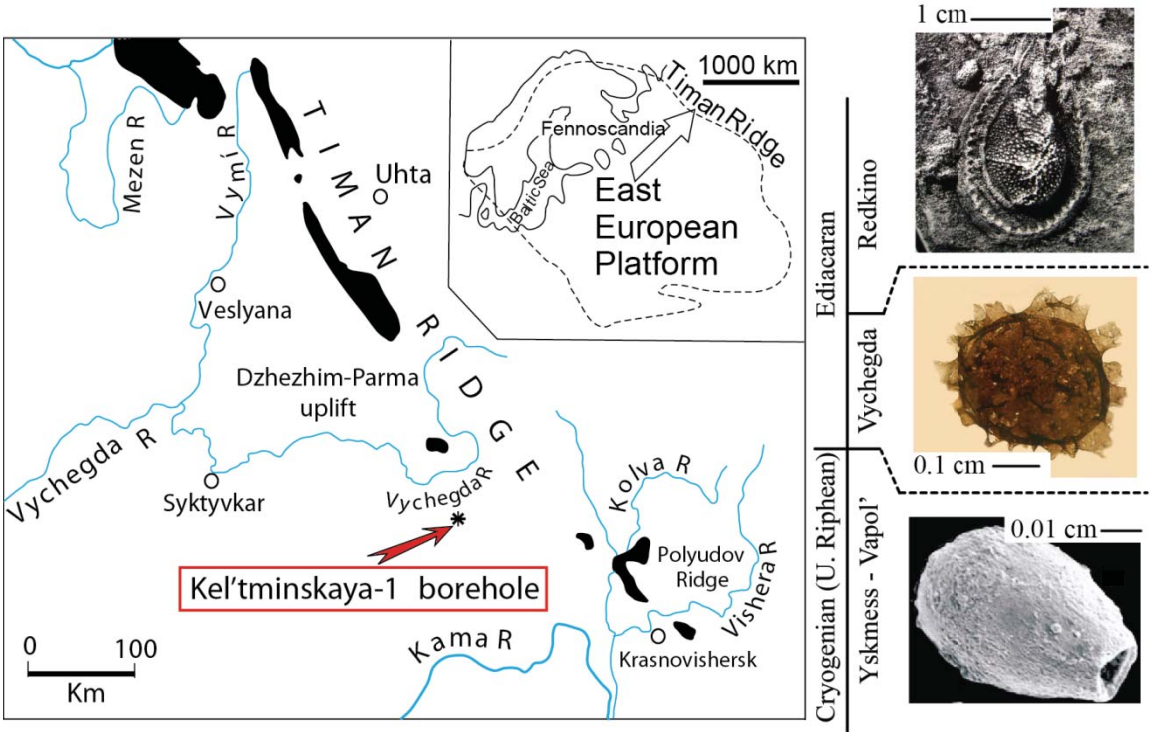

Figure 2: Stratigraphic redox proxy variations for the Kel'tminskaya-1 drillhole. Note the break in vertical scale at the Vapol'–Vychegda sequence boundary. The age of deposition is based on lithological and biostratigraphic correlation to the White Sea and Ural Mountains successions. Note that the 635 Ma age relates to the strata underlying the hiatus in the lower Vychegda, whereas the ~580 Ma age relates to that of the overlying ECAP-containing portion of the unit. All methods and additional data are described in the text and presented in the supplemental materials. The two leftmost chemostratigraphic frames are on a log scale. Vertical lines in the FeHr/FeT column are discussed in the text, with red circles with lines extending horizontally representing samples with FeHr/FeT > 0.6 and indicate anoxia. Where indicating anoxia, all samples are ferruginous. Carbon isotope axes for carbonate and organic carbon (far right panel) are offset by 31‰.

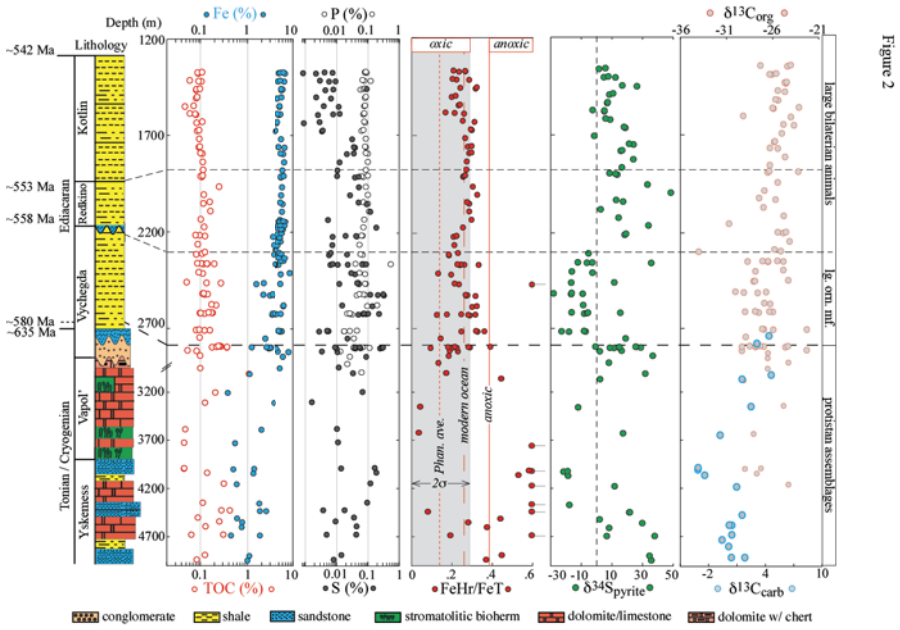

Figure 2

554

555 **Figure 3:** Two frames indicating the relationship between FeHr/FeT (a measure of anoxia)
556 versus **(a)** top: a quantification of pyrite iron, Fe_{py}/FeHr and **(b)** bottom: an alternative means of
557 recording anoxia. A key to the symbols is listed under the figure, with all data coming from this
558 work. In **(a)**, regions of the plot characteristic of particular water column redox state and
559 chemistry are noted. That is, FeHr/FeT > 0.38 is indicative of anoxia, whereas values below the
560 modern average (0.26) are indicative of oxic conditions (Anderson and Raiswell, 2004; Poulton
561 and Canfield, 2011; Poulton and Raiswell, 2002; Raiswell and Canfield, 1998). The hashed
562 region, between these two values, carries a more equivocal meaning. For reference, the
563 Phanerozoic average for shale is also listed (dashed line). In frame **(b)**, the crustal average of
564 Fe/Al is indicated. See text for further discussions, especially that of the Vapol' and Yskemess
565 formation carbonates.

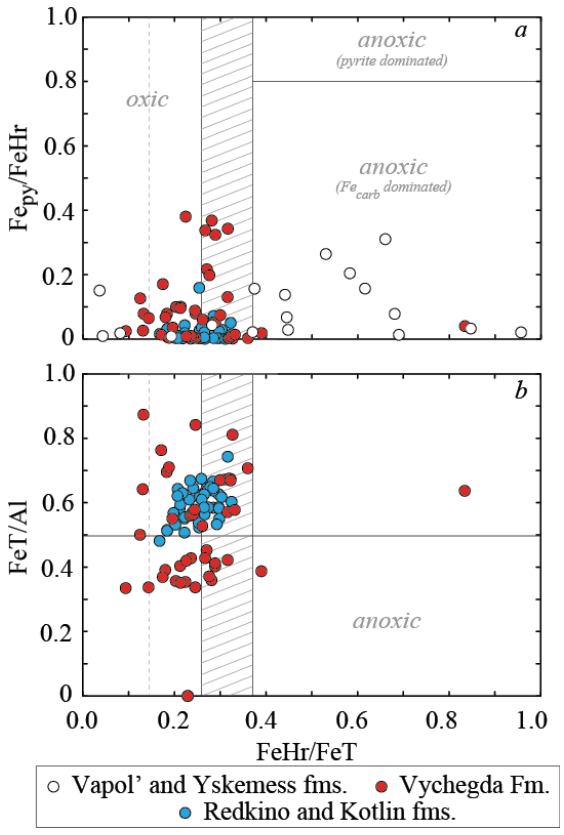

566

Figure 4: A summary of Fe-speciation data for pre-Sturtian sediments from Russia (this work), North America (Johnston et al., 2010), East Greenland, and Australia (Canfield et al., 2008). Axes are the same as Figure 3a, as are distinctions in FeHr/FeT.

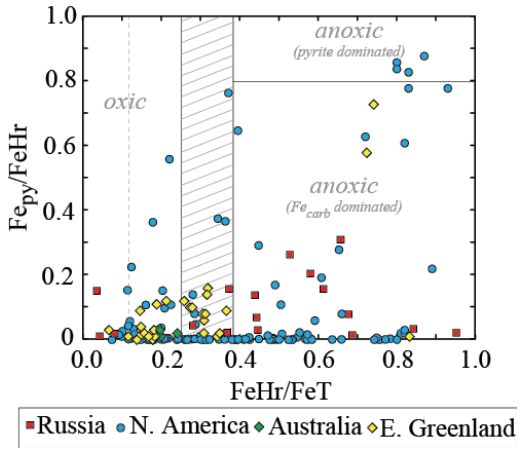

Figure 5: An analysis of the covariance between different biogeochemical metrics. Here, we examine changes in TOC against **(a)** reactive iron to total iron ratios, and **(b)** versus total P content. Both figures are also contoured by lines representing different ratios between the abscissa and ordinate measures. These features are fully described in the text and both relate to oxygen content of the local environment.

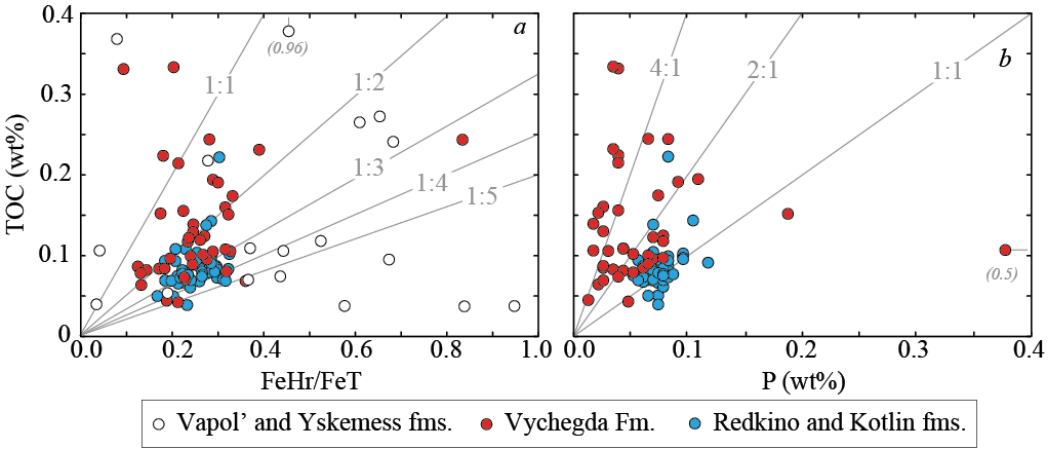

Figure 6: A statistical resampling of key geochemical metrics from the Ediacaran of the EEP. Data sets were divided at the Vychegda-Redkino sequence boundary (Vychegda in blue, Redkino and Kotlin in red). Importantly, sampling of the Vychegda began at 2779 m, the bed at which distinctly Ediacaran acritarchs first appear (Vorob'eva et al., 2009a). **a)** A measure of overall water column redox, FeHr/FeT. **b)** The relationship between Fe and Al. **c)** The chemical index of alteration is described in the text. **d)** The isotopic composition of pyrite sulfur. In all cases, one thousand synthetic runs were performed (binned and recorded on ordinate axis). Ordinate axis scale changes from frame to frame.

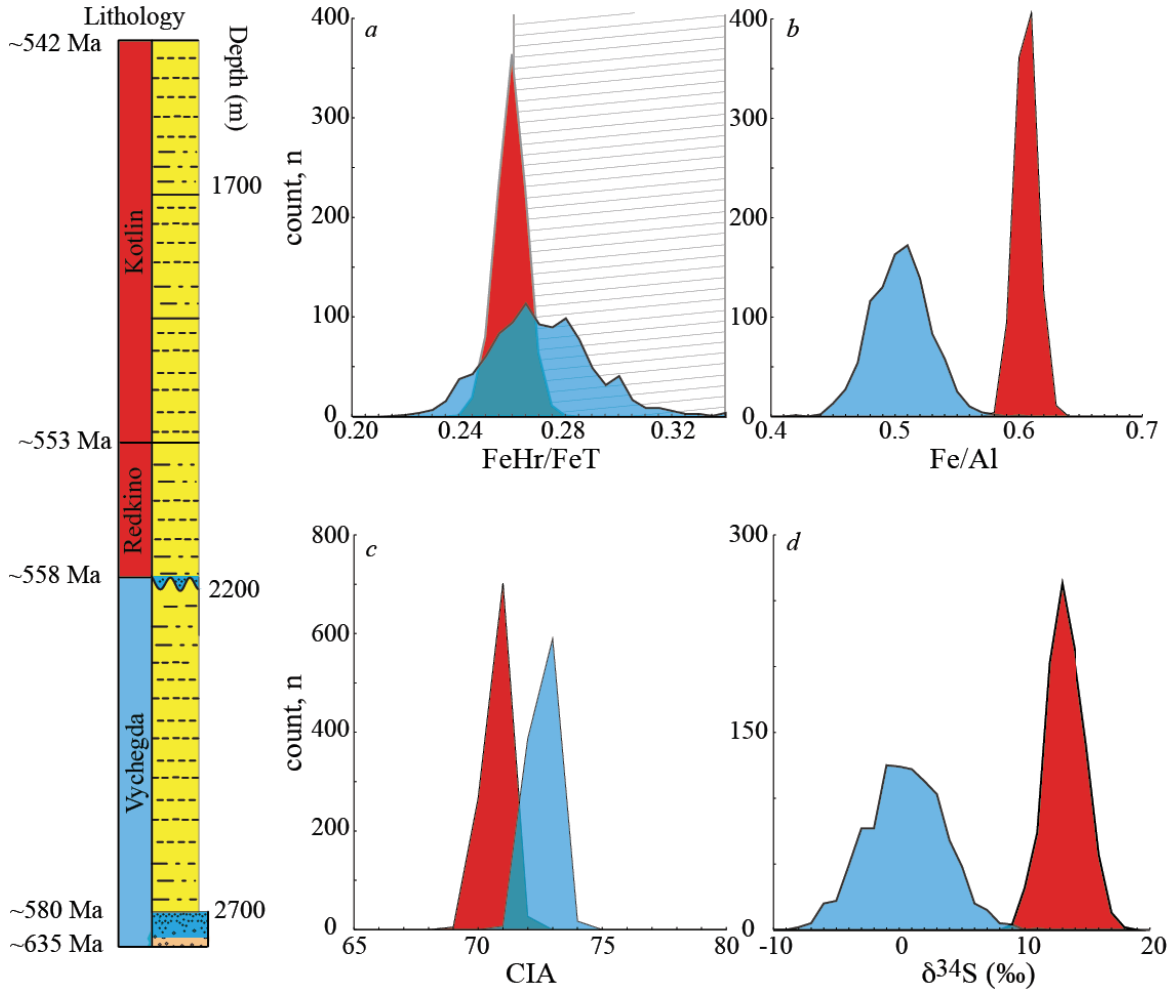

586 **Figure 7:** Two plots examining the relationship between the sulfur isotopic composition of
587 pyrite and **(a)** reactive to total iron ratio (FeHr/FeT) and **(b)** total organic carbon content, TOC.
588 Symbols are described below the figure, and the data is discussed in the text.

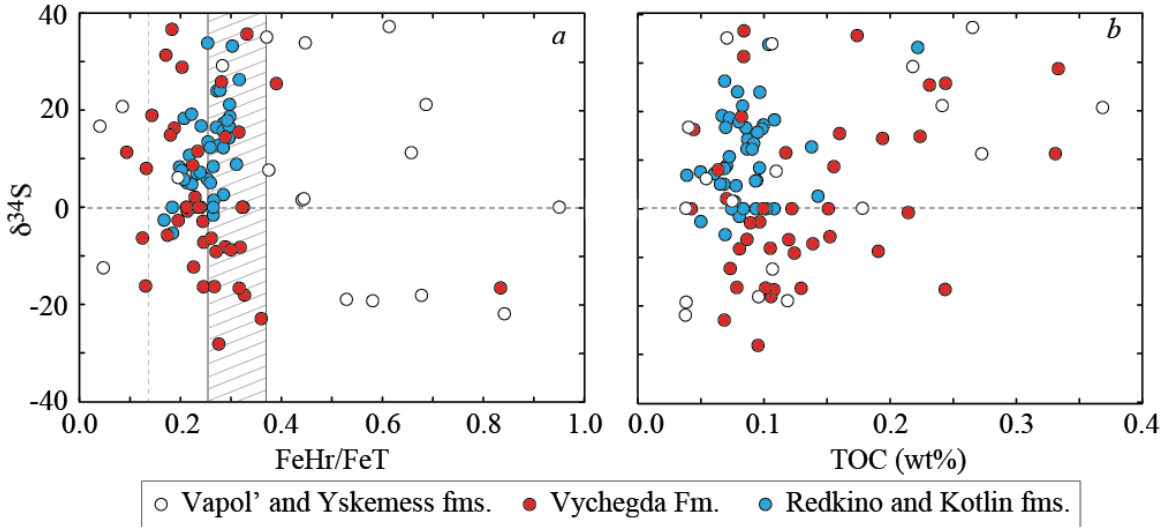

589

590

590 REFERENCE LIST:

591 Algeo, T.J., Ingall, E., 2007. Sedimentary C_{org}: P ratios, paleocean ventilation, and
592 Phanerozoic atmospheric pO_2. Palaeogeography Palaeoclimatology Palaeoecology 256,
593 130-155.
594 Anderson, T.F., Raiswell, R., 2004. Sources and mechanisms for the enrichment of highly
595 reactive iron in euxinic Black Sea sediments. American Journal of Science 304, 203-233.
596 Bartley, J.K., Semikhatov, M.A., Kaufman, A.J., Knoll, A.H., Pope, M.C., Jacobsen, S.B., 2001.
597 Global events across the Mesoproterozoic-Neoproterozoic boundary: C and Sr isotopic
598 evidence from Siberia. Precambrian Research 111, 165-202.
599 Bengston, S., Morris, S.C., 1992. Early radiation of biomineralizing phyla. Topics in
600 Geobiology 10, 447-481.
601 Bergman, N.M., Lenton, T.M., Watson, A.J., 2004. COPSE: A new model of biogeochemical
602 cycling over Phanerozoic time. American Journal of Science 304, 397-437.
603 Berner, R.A., Canfield, D.E., 1989. A new model for atmospheric oxygen over Phanerozoic
604 time. American Journal of Science 289, 333-361.
605 Bingen, B., Griffin, W.L., Torsvik, T.H., Saeed, A., 2005. Timing of Late Neoproterozoic
606 glaciation on Baltica constrained by detrital zircon geochronology in the Hedmark Group,
607 south-east Norway. Terra Nova 17, 250-258.
608 Butterfield, N.J., 2007. Macroevolution and macroecology through deep time. Palaeontology
609 50, 41-55.
610 Butterfield, N.J., 2009. Oxygen, animals and oceanic ventilation: an alternative view.
611 Geobiology 7, 1-7.

612 Canfield, D.E., 2001. Biogeochemistry of sulfur isotopes, Stable Isotope Geochemistry, pp.
613 607-636.
614 Canfield, D.E., Lyons, T.W., Raiswell, R., 1996. A model for iron deposition to euxinic Black
615 Sea sediments. American Journal of Science 296, 818-834.
616 Canfield, D.E., Poulton, S.W., Knoll, A.H., Narbonne, G.M., Ross, G., Goldberg, T., Strauss, H.,
617 2008. Ferruginous conditions dominated later neoproterozoic deep-water chemistry.
618 Science 321, 949-952.
619 Canfield, D.E., Poulton, S.W., Narbonne, G.M., 2007. Late-Neoproterozoic deep-ocean
620 oxygenation and the rise of animal life. Science 315, 92-95.
621 Canfield, D.E., Raiswell, R., Bottrell, S., 1992. The reactvity of sedimentary iron minerals
622 towards sulfide. American Journal of Science 292, 659-683.
623 Canfield, D.E., Raiswell, R., Westrich, J.T., Reaves, C.M., Berner, R.A., 1986. The use of
624 chromium reduction in the analysis of reduced inorganic sulfurin sediments and shales.
625 Chemical Geology 54, 149-155.
626 Canfield, D.E., Teske, A., 1996. Late Proterozoic rise in atmospheric oxygen concentration
627 inferred from phylogenetic and sulphur-isotope studies. Nature 382, 127-132.
628 Claypool, G.E., Holser, W.T., Kaplan, I.R., Sakai, H., Zak, I., 1980. The age curves of sulfur and
629 oxygen isotopes in marine sulfate and their mutual interpretation. Chemical Geology 28,
630 199-260.
631 Cloud, P.E., Drake, E.T., 1968. Pre-metazoan evolution and the origins of the Metazoa.
632 Evolution and environment: a symposium., 1-72.

633 Cohen, P.A., Knoll, A.H., Kodner, R.B., 2009. Large spinose microfossils in Ediacaran rocks as
634 resting stages of early animals. Proceedings of the National Academy of Sciences of the
635 United States of America 106, 6519-6524.
636 Dahl, T.W., Hammarlund, E.U., Anbar, A.D., Bond, D.P.G., Gill, B.C., Gordon, G.W., Knoll, A.H.,
637 Nielsen, A.T., Schovsbo, N.H., Canfield, D.E., 2010. Devonian rise in atmospheric oxygen
638 correlated to the radiations of terrestrial plants and large predatory fish. Proceedings of the
639 National Academy of Sciences of the United States of America 107, 17911-17915.
640 Diaz, R.J., Rosenberg, R., 1995. Marine benthic hypoxia: A review of its ecological effects and
641 the behavioural responses of benthic macrofauna, in: Ansell, A.D., Gibson, R.N., Barnes, M.
642 (Eds.), Oceanography and Marine Biology - an Annual Review, Vol 33, pp. 245-303.
643 Erwin, D.H., Laflamme, M., Tweedt, S.M., Sperling, E.A., Pisani, D., Peterson, K.J., 2011. The
644 Cambrian Conundrum: Early Divergence and Later Ecological Success in the Early History
645 of Animals. Science 334, 1091-1097.
646 Fedonkin, M., Simonetta, A., Ivantsov, A.Y., 2007. New data on Kimberella, the Vendian
647 mollusc-like organism (White Sea region, Russia): palaeoecological and evolutionary
648 implications. Geological Society Special Publication 286, 157-179.
649 Fedonkin, M.A., Waggoner, B.M., 1997. The Late Precambrian fossil Kimberella is a mollusc-
650 like bilaterian organism. Nature 388, 868-871.
651 Fike, D.A., Grotzinger, J.P., 2008. A paired sulfate-pyrite $\delta^{34}S$ approach to understanding the
652 evolution of the Ediacaran-Cambrian sulfur cycle. Geochimica Et Cosmochimica Acta 72,
653 2636-2648.
654 Fike, D.A., Grotzinger, J.P., Pratt, L.M., Summons, R.E., 2006. Oxidation of the Ediacaran
655 Ocean. Nature 444, 744-747.

656 Garrels, R.M., Lerman, A., 1981. Phanerozoic cycles of sedimentary carbon and sulfur.
657 Proceedings of the National Academy of Sciences of the United States of America-Physical
658 Sciences 78, 4652-4656.
659 Goldberg, T., Poulton, S.W., Strauss, H., 2005. Sulphur and oxygen isotope signatures of late
660 Neoproterozoic to early Cambrian sulphate, Yangtze Platform, China: Diagenetic
661 constraints and seawater evolution. Precambrian Research 137, 223-241.
662 Grazhdankin, D.V., 2003. Structure and depositional environment of the Vendian Complex
663 in the southeastern White Sea area. Stratigraphy and Geological Correlation 11, 313-331.
664 Grey, K., 2005. Ediacaran palynology of Australia. Memoirs of the Association of
665 Australasian Palaeontologists 31, 1-439.
666 Grey, K., Calver, C.R., 2007. Correlating the Ediacaran of Australia. Geological Society Special
667 Publication 286, 115-135.
668 Grey, K., Walter, M.R., Calver, C.R., 2003. Neoproterozoic biotic diversification: Snowball
669 Earth or aftermath of the Acraman impact? Geology 31, 459-462.
670 Habicht, K.S., Gade, M., Thamdrup, B., Berg, P., Canfield, D.E., 2002. Calibration of sulfate
671 levels in the Archean Ocean. Science 298, 2372-2374.
672 Halverson, G.P., Hurtgen, M.T., 2007. Ediacaran growth of the marine sulfate reservoir.
673 Earth and Planetary Science Letters 263, 32-44.
674 Hayes, J.M., 2001. Fractionation of carbon and hydrogen isotopes in biosynthetic processes,
675 Stable Isotope Geochemistry, pp. 225-277.
676 Hayes, J.M., Strauss, H., Kaufman, A.J., 1999. The abundance of ^{13}C in marine organic matter
677 and isotopic fractionation in the global biogeochemical cycle of carbon during the past 800
678 Ma. Chemical Geology 161, 103-125.

679 Hedges, J.I., Keil, R.G., 1995. Sedimentary organic matter preservation - an assessment and
680 speculative synthesis. Marine Chemistry 49, 81-115.
681 Hoffman, P.F., Kaufman, A.J., Halverson, G.P., Schrag, D.P., 1998. A Neoproterozoic snowball
682 earth. Science 281, 1342-1346.
683 Hurtgen, M.T., Arthur, M.A., Suits, N.S., Kaufman, A.J., 2002. The sulfur isotopic composition
684 of Neoproterozoic seawater sulfate: implications for a snowball Earth? Earth and Planetary
685 Science Letters 203, 413-429.
686 Hurtgen, M.T., Halverson, G.P., Arthur, M.A., Hoffman, P.F., 2006. Sulfur cycling in the
687 aftermath of a 635-Ma snowball glaciation: Evidence for a syn-glacial sulfidic deep ocean.
688 Earth and Planetary Science Letters 245, 551-570.
689 Ingall, E., Jahnke, R., 1994. Evidence for enhanced phosphorus regeneration from marine
690 sediments overlain by oxygen depleted waters. Geochimica Et Cosmochimica Acta 58,
691 2571-2575.
692 Jiang, G., Kaufman, A.J., Christie-Blick, N., Zhang, S., Wu, H., 2007. Carbon isotope variability
693 across the Ediacaran Yangtze platform in South China: Implications for a large surface-to-
694 deep ocean delta C-13 gradient. Earth and Planetary Science Letters 261, 303-320.
695 Jilbert, T., Slomp, C.P., Gustafsson, B.G., Boer, W., 2011. Beyond the Fe-P-redox connection:
696 preferential regeneration of phosphorus from organic matter as a key control on Baltic Sea
697 nutrient cycles. Biogeosciences 8, 1699-1720.
698 Johnston, D.T., 2011. Multiple sulfur isotopes and the evolution of Earth's surface sulfur
699 cycle. Earth-Science Reviews 106, 161-183.
700 Johnston, D.T., Macdonald, F.A., Gill, B.C., Hoffman, P.F., Schrag, D.P., 2012. Uncovering the
701 Neoproterozoic carbon cycle. Nature 483, 320-U110.

Johnston, D.T., Poulton, S.W., Dehler, C., Porter, S., Husson, J., Canfield, D.E., Knoll, A.H., 2010. An emerging picture of Neoproterozoic ocean chemistry: Insights from the Chuar Group, Grand Canyon, USA. Earth and Planetary Science Letters 290, 64-73.

Johnston, D.T., Wing, B.A., Farquhar, J., Kaufman, A.J., Strauss, H., Lyons, T.W., Kah, L.C., Canfield, D.E., 2005. Active microbial sulfur disproportionation in the Mesoproterozoic. Science 310, 1477-1479.

Kah, L.C., Bartley, J.K., 2011. Protracted oxygenation of the Proterozoic biosphere. International Geology Review 53, 1424-1442.

Kampschulte, A., Strauss, H., 2004. The sulfur isotopic evolution of Phanerozoic seawater based on the analysis of structurally substituted sulfate in carbonates. Chemical Geology 204, 255-286.

Kaufman, A.J., Jiang, G.Q., Christie-Blick, N., Banerjee, D.M., Rai, V., 2006. Stable isotope record of the terminal Neoproterozoic Krol platform in the Lesser Himalayas of northern India. Precambrian Research 147, 156-185.

Keil, R.G., Montlucon, D.B., Prahl, F.G., Hedges, J.I., 1994. Sorptive preservation of labile organic matter in marine sediments. Nature 370, 549-552.

Kendall, B., Reinhard, C.T., Lyons, T., Kaufman, A.J., Poulton, S.W., Anbar, A.D., 2010. Pervasive oxygenation along late Archaean ocean margins. Nature Geoscience 3, 647-652.

Kennedy, M., Droser, M., Mayer, L.M., Pevear, D., Mrofka, D., 2006. Late Precambrian oxygenation; Inception of the clay mineral factory. Science 311, 1446-1449.

Knoll, A.H., 1994. Proterozoic and early Cambrian protists - evidence for accelerating evolutionary tempo. Proceedings of the National Academy of Sciences of the United States of America 91, 6743-6750.

725 Knoll, A.H., 2011. The Multiple Origins of Complex Multicellularity, in: Jeanloz, R.F.K.H.
726 (Ed.), Annual Review of Earth and Planetary Sciences, Vol 39, pp. 217-239.
727 Knoll, A.H., Hayes, J.M., Kaufman, A.J., Swett, K., Lambert, I.B., 1986. Secular variation in
728 carbon isotope ratios from upper Proterozoic successions of Svalbard and east Greenland.
729 Nature 321, 832-838.
730 Kraal, P., Slomp, C.P., de Lange, G.J., 2010. Sedimentary organic carbon to phosphorus ratios
731 as a redox proxy in Quaternary records from the Mediterranean. Chemical Geology 277,
732 167-177.
733 Levin, L.A., 2003. Oxygen minimum zone benthos: Adaptation and community response to
734 hypoxia. Oceanography and Marine Biology, Vol 41 41, 1-45.
735 Li, C., Love, G.D., Lyons, T.W., Fike, D.A., Sessions, A.L., Chu, X.L., 2010. A Stratified Redox
736 Model for the Ediacaran Ocean. Science 328, 80-83.
737 Logan, G.A., Hayes, J.M., Hieshima, G.B., Summons, R.E., 1995. Terminal Proterozoic
738 reorganization of biogeochemical cycles. Nature 376, 53-56.
739 Lyons, T.W., Severmann, S., 2006. A critical look at iron paleoredox proxies: New insights
740 from modern euxinic marine basins. Geochimica Et Cosmochimica Acta 70, 5698-5722.
741 Lyons, T.W., Werne, J.P., Hollander, D.J., Murray, R.W., 2003. Contrasting sulfur
742 geochemistry and Fe/Al and Mo/Al ratios across the last oxic-to-anoxic transition in the
743 Cariaco Basin, Venezuela. Chemical Geology 195, 131-157.
744 Martin, M.W., Grazhdankin, D.V., Bowring, S.A., Evans, D.A.D., Fedonkin, M.A., Kirschvink,
745 J.L., 2000. Age of Neoproterozoic bilatarian body and trace fossils, White Sea, Russia:
746 Implications for metazoan evolution. Science 288, 841-845.

747 Marz, C., Poulton, S.W., Beckmann, B., Kuster, K., Wagner, T., Kasten, S., 2008. Redox
748 sensitivity of P cycling during marine black shale formation: Dynamics of sulfidic and
749 anoxic, non-sulfidic bottom waters. Geochimica Et Cosmochimica Acta 72, 3703-3717.
750 Maslov, A., ZM, A., LA, K., VN, P., 1994. First finds of melancyrilliums in Riphean type
751 section, southern Ural Mountains, The results, problems and perspectives of the
752 Precambrian deposits, areas, geological mapping on the territory of Russia, p. 90.
753 McFadden, K.A., Huang, J., Chu, X.L., Jiang, G.Q., Kaufman, A.J., Zhou, C.M., Yuan, X.L., Xiao,
754 S.H., 2008. Pulsed oxidation and bioloical evolution in the Ediacaran Doushantuo
755 Formation. Proceedings of the National Academy of Sciences of the United States of
756 America 105, 3197-3202.
757 Narbonne, G.M., 2005. The ediacarabiota: Neoproterozoic origin of animals and their
758 ecosystems. Annual Review of Earth and Planetary Sciences 33, 421-442.
759 Narbonne, G.M., Aitken, J.D., 1990. Ediacaran fossils from the Sekwi Brook area, Mackenzie
760 Mountains, northwest Canada. Palaeontology 33, 945-980.
761 Nesbitt, H.W., Fedo, C.M., Young, G.M., 1997. Quartz and feldspar stability, steady and non-
762 steady-state weathering, and petrogenesis of siliciclastic sands and muds. Journal of
763 Geology 105, 173-191.
764 Nesbitt, H.W., Young, G.M., 1984. Preictions of some weathering trends of plutonic and
765 volcanic rocks based on thermodynamic and kinetic considerations. Geochimica Et
766 Cosmochimica Acta 48, 1523-1534.
767 Nesbitt, H.W., Young, G.M., McLennan, S.M., Keays, R.R., 1996. Effects of chemical
768 weathering and sorting on the petrogenesis of siliciclastic sediments, with implications for
769 provenance studies. Journal of Geology 104, 525-542.

770 Nursall, J.R., 1959. Oxygen as a prerequisite to the origin of the Metazoa. Nature 183, 1170-
771 1172.
772 Ovchinnikova, G.V., Vasil'eva, I.M., Semikhatov, M.A., Gorokhov, I.M., Kuznetsov, A.B.,
773 Gorokhovskii, B.M., Levskii, L.K., 2000. The Pb-Pb trail dating of carbonates with open U-Pb
774 systems: The Min'yar Formation of the Upper Riphean stratotype, southern Urals.
775 Stratigraphy and Geological Correlation 8, 529-543.
776 Payne, J.L., McClain, C.R., Boyer, A.G., Brown, J.H., Finnegan, S., Kowalewski, M., Krause, R.A.,
777 Lyons, S.K., McShea, D.W., Novack-Gottshall, P.M., Smith, F.A., Spaeth, P., Stempien, J.A.,
778 Wang, S.C., 2011. The evolutionary consequences of oxygenic photosynthesis: a body size
779 perspective. Photosynthesis Research 107, 37-57.
780 Peterson, K.J., Butterfield, N.J., 2005. Origin of the Eumetazoa: Testing ecological
781 predictions of molecular clocks against the Proterozoic fossil record. Proceedings of the
782 National Academy of Sciences of the United States of America 102, 9547-9552.
783 Podkovyrov, V.N., Semikhatov, M.A., Kuznetsov, A.B., Vinogradov, D.P., Kozlov, V.I., Kislova,
784 I.V., 1998. Carbonate carbon isotopic composition in the upper Riphean stratotype, the
785 Karatau group, southern Urals. Stratigraphy and Geological Correlation 6, 319-335.
786 Pokrovskii, B.G., Melezhik, V.A., Bujakaite, M.I., 2006. Carbon, Oxygen, Strontium and Sulfur
787 isotopic compositons in Late Precambrian Rocks of the Patom Complex, Central Siberia.
788 Lithology and Mineral Resources, 450-474.
789 Porter, S.M., Meisterfeld, R., Knoll, A.H., 2003. Vase-shaped microfossils from the
790 Neoproterozoic Chuar Group, Grand Canyon: A classification guided by modern testate
791 amoebae. Journal of Paleontology 77, 409-429.

792 Poulton, S.W., Canfield, D.E., 2005. Development of a sequential extraction procedure for
793 iron: implications for iron partitioning in continentally derived particulates. Chemical
794 Geology 214, 209-221.
795 Poulton, S.W., Canfield, D.E., 2011. Ferruginous Conditions: A Dominant Feature of the
796 Ocean through Earth's History. Elements 7, 107-112.
797 Poulton, S.W., Fralick, P.W., Canfield, D.E., 2004a. The transition to a sulphidic ocean similar
798 to 1.84 billion years ago. Nature 431, 173-177.
799 Poulton, S.W., Krom, M.D., Raiswell, R., 2004b. A revised scheme for the reactivity of iron
800 (oxyhydr)oxide minerals towards dissolved sulfide. Geochimica Et Cosmochimica Acta 68,
801 3703-3715.
802 Poulton, S.W., Raiswell, R., 2002. The low-temperature geochemical cycle of iron: From
803 continental fluxes to marine sediment deposition. American Journal of Science 302, 774-
804 805.
805 Raaben, M.E., Oparenkova, L.I., 1997. New data on the Riphean stratigraphy of Timan.
806 Stratigraphy and Geological Correlation 5, 110-117.
807 Raff, R.A., Raff, E.C., 1970. Respiratory mechanisms and metazoan fossil record. Nature 228,
808 1003-&.
809 Raiswell, R., Buckley, F., Berner, R.A., Anderson, T.F., 1988. Degree of pyritization of iron as
810 a paleoenvironmental indicator of bottom water oxygenation. Journal of Sedimentary
811 Petrology 58, 812-819.
812 Raiswell, R., Canfield, D.E., 1996. Rates of reaction between silicate iron and dissolved
813 sulfide in Peru Margin sediments. Geochimica Et Cosmochimica Acta 60, 2777-2787.

814 Raiswell, R., Canfield, D.E., 1998. Sources of iron for pyrite formation in marine sediments.
815 American Journal of Science 298, 219-245.
816 Raiswell, R., Canfield, D.E., Berner, R.A., 1994. A comparison of iron extraction methods for
817 the determination of degree of pyritization and the recognition of iron limited pyrite
818 formation. Chemical Geology 111, 101-110.
819 Raiswell, R., Newton, R., Wignall, P.B., 2001. An indicator of water-column anoxia:
820 Resolution of biofacies variations in the Kimmeridge Clay (Upper Jurassic, UK). Journal of
821 Sedimentary Research 71, 286-294.
822 Rhoads, D.C., Morse, J.W., 1971. Evolutionary and ecologic significance of oxygen deficient
823 marine basins. Lethaia 4, 413-&.
824 Ries, J.B., Fike, D.A., Pratt, L.M., Lyons, T.W., Grotzinger, J.P., 2009. Superheavy pyrite (delta
825 S-34(pyr) > delta S-34(CAS)) in the terminal Proterozoic Nama Group, southern Namibia: A
826 consequence of low seawater sulfate at the dawn of animal life. Geology 37, 743-746.
827 Rothman, D.H., Forney, D.C., 2007. Physical model for the decay and preservation of marine
828 organic carbon. Science 316, 1325-1328.
829 Runnegar, B., 1991. Precambrian oxygen levels estimated from the biochemistry and
830 physiology of early eukaryotes. Palaeogeography Palaeoclimatology Palaeoecology 97, 97-
831 111.
832 Scott, C., Lyons, T.W., Bekker, A., Shen, Y., Poulton, S.W., Chu, X., Anbar, A.D., 2008. Tracing
833 the stepwise oxygenation of the Proterozoic ocean. Nature 452, 456-U455.
834 Seibel, B.A., Drazen, J.C., 2007. The rate of metabolism in marine animals: environmental
835 constraints, ecological demands and energetic opportunities. Philosophical Transactions of
836 the Royal Society B-Biological Sciences 362, 2061-2078.

837 Sergeev, V.N., Precambrian microfossils in cherts: their paleobiology, classification, and
838 biostratigraphic usefulness. GEOS, Moscow, p. 280.
839 Sergeev, V.N., 2006. Precambrian microfossils in cherts: their paleobiology, classification,
840 and biostratigraphic usefulness. GEOS, Moscow, p. 280.
841 Sergeev, V.N., Knoll, A.H., Vorob'eva, N.G., 2011. Ediacaran microfossils from the Ura
842 Formation, Baikal-Patom uplift, Siberia: Taxonomy and Biostratigraphic significance.
843 Journal of Paleontology 85, 987-1011.
844 Sergeev, V.N., Seong-Joo, L., 2006. Real eukaryotes and precipitates first found in the Middle
845 Riphean stratotype, southern Urals. Stratigraphy and Geological Correlation 14, 1-18.
846 Severmann, S., Lyons, T.W., Anbar, A., McManus, J., Gordon, G., 2008. Modern iron isotope
847 perspective on the benthic iron shuttle and the redox evolution of ancient oceans. Geology
848 36, 487-490.
849 Shen, Y.N., Zhang, T.G., Hoffman, P.F., 2008. On the coevolution of Ediacaran oceans and
850 animals. Proceedings of the National Academy of Sciences of the United States of America
851 105, 7376-7381.
852 Sokolov, B.S., Fedonkin, M.A., 1990. The Vendian System. Springer-Verlag, Berlin.
853 Sokolov, B.S., Iwanowski, A.B., 1990. The Vendian System: Paleontology, The Vendian
854 System. Springer-Verlag, Berlin.
855 Sperling, E.A., Vinther, J., 2010. A placozoan affinity for Dickinsonia and the evolution of late
856 Proterozoic metazoan feeding modes. Evolution & Development 12, 201-209.
857 Stanley, S.M., 1973. Ecological theory for sudden origin of multicellular life in late
858 Precambrian . Proceedings of the National Academy of Sciences of the United States of
859 America 70, 1486-1489.

860 Swanson-Hysell, N.L., Rose, C.V., Calmet, C.C., Halverson, G.P., Hurtgen, M.T., Maloof, A.C.,
861 2010. Cryogenian Glaciation and the Onset of Carbon-Isotope Decoupling. Science 328, 608-
862 611.
863 Tosca, N.J., Johnston, D.T., Mushegian, A., Rothman, D.H., Summons, R.E., Knoll, A.H., 2010.
864 Clay mineralogy, organic carbon burial, and redox evolution in Proterozoic oceans.
865 Geochimica Et Cosmochimica Acta 74, 1579-1592.
866 Turekian, K.K., Wedepohl, K.H., 1961. Distribution of the elements in some major units of
867 the Earth's crust. Geological Society of America Bulletin 72, 175-191.
868 Vaquer-Sunyer, R., Duarte, C.M., 2008. Thresholds of hypoxia for marine biodiversity.
869 Proceedings of the National Academy of Sciences of the United States of America 105,
870 15452-15457.
871 Vorob'eva, N.G., Sergeev, V.N., Knoll, A.H., 2009a. Neoproterozoic microfossils from the
872 margin of the East European Platform and the search for a biostratigraphic model of lower
873 Ediacaran rocks. Precambrian Research 173, 163-169.
874 Vorob'eva, N.G., Sergeev, V.N., Knoll, A.H., 2009b. Neoproterozoic microfossils from the
875 northeastern margin of the East European Platform. Journal of Paleontology 83, 161-196.
876 Yin, L.M., Zhu, M.Y., Knoll, A.H., Yuan, X.L., Zhang, J.M., Hu, J., 2007. Doushantuo embryos
877 preserved inside diapause egg cysts. Nature 446, 661-663.
878 Yuan, X.L., Chen, Z., Xiao, S.H., Zhou, C.M., Hua, H., 2011. An early Ediacaran assemblage of
879 macroscopic and morphologically differentiated eukaryotes. Nature 470, 389-392.

880

881

HARVARD UNIVERSITY
DEPARTMENT OF EARTH AND PLANETARY SCIENCES
20 OXFORD ST.
CAMBRIDGE, MA 02138
TEL. (617) 495-2351 FAX. (617) 495-8839

Highlights for *Late Ediacaran redox stability and metazoan evolution* by Johnston *et al.*

1) Redox stability, in addition to O_2, is critical for animal evolution.

2) We explain Ediacaran global asynchroneity in sedimentary proxy and animals records.

3) We revisit the importance of dysoxia for biological evolution.

4) The data reinforce that Ediacaran acritarchs are resting stages of early animals.